Molecular Spin-Flip Loss and a Dual Quadrupole Trap

David Reens,* Hao Wu,* Tim Langen,† and Jun Ye
JILA, National Institute of Standards and Technology and the University of Colorado and Department of Physics, University of Colorado, Boulder, Colorado 80309-0440, USA
(Dated: May 2, 2017)

Doubly dipolar molecules exhibit complex internal spin-dynamics when electric and magnetic fields are both applied. Near magnetic trap minima, these spin-dynamics lead to enhancements in Majorana spin-flip transitions by many orders of magnitude relative to atoms, and are thus an important obstacle for progress in molecule trapping and cooling. The effect is strongest for Hund's case (a) states and is significant for Hund's case (b) as well. We study these internal spin-dynamics with OH molecules and devise a trap geometry where spin-flip loss can be tuned from over 200 s^{-1} to complete removal with only a weak external bias coil and with no sacrifice of trap strength.

The ultracold regime extends toward molecules on many fronts [1]. KRb molecules have reached lattice quantum degeneracy [2] and other bialkalis continue to progress [3–6]. Creative and carefully engineered laser cooling strategies are tackling certain nearly vibrationally diagonal molecules [7–11]. A diverse array of alternative strategies have succeeded to greater or lesser extents on other molecules [12–18]. All of these molecules will require secondary strategies like evaporation or sympathetic cooling to make further gains in phase space density [19–21]. They also may face a familiar challenge: spin flip loss near the zero of a magnetic trap, but dramatically enhanced for many doubly dipolar molecules due to their internal spin dynamics in mixed electric and magnetic fields.

The knowledge of spin flips or Majorana hops as an eventual trap lifetime limit predates the very first magnetic trapping of neutrals [22]. Spin flips were directly observed near 50 μK and overcome with a time-orbiting potential trap [23] and a plugged dipole trap [24], famously enabling the first production of Bose-Einstein condensates. In our earlier investigations, we observed loss of magnetically trapped hydroxyl radicals (OH) with applied electric field [25]. This trap loss occurred for substates of OH's $X^2\Pi_{J=3/2}$ ground state manifold other than the doubly weak-field seeking one of positive parity and full spin polarization, the $|f, m_J = 3/2\rangle$ state, colored blue in Fig. 1. These other states intersect levels of opposite parity at non-zero magnetic fields, where electric field can open avoided crossings and cause trap loss. We now identify internal spin-dynamics leading to trap loss near zero B-field for the $|f, 3/2\rangle$ state even at 50 mK and more strongly below.

These internal spin-dynamics are subtle, having eluded three previous investigations of note: In [26] the analogues of atomic spin-flip loss for molecules in mixed fields were modeled, and a magnetic quadrupole trap for OH molecules with superposed electric field was specifically addressed. It was concluded that no significant loss enhancement due to electric field would be evident. This is true only for the approximate $^2\Pi_{1/2}$ Hamiltonian used in that study. In [27] E-fields were applied in our magnetic quadrupole trap to study E-field induced collisions. Although an initial approximation was made of the spin-dynamical effect, subsequent investigations have revealed it to be a threefold underestimate, enough to render deconvolution of any remaining collisional effect difficult. Finally, in [28] it was correctly noted that Hund's case (a) molecules maintain a quantization axis in mixed fields. The states of the molecule were shown to align with one of two quantization axes- either the vector sum or the vector difference of the dipole moment weighted fields $\mu_E\vec{E}$ and $\mu_B\vec{B}$. It was asserted that this would maintain quantization near the zero of a quadrupole trap and avoid spin-flip loss. As we now explain and demonstrate with conclusive experimental evidence, quantization is indeed maintained, but spin-flip loss is enhanced.

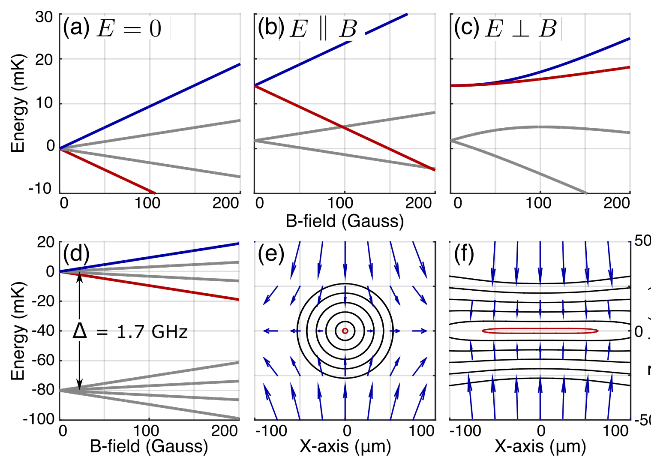

FIG. 1. Four Zeeman split lines in OH's $J = 3/2$ ground manifold are shown (a-c), with the trapped $|f, 3/2\rangle$ state in blue and its spin-flip partner $|f, -3/2\rangle$ in red. These states are shown with no E-field (a), with $E = 150$ V/cm and $E \parallel B$ (b), and with $E \perp B$ (c). Note the vastly reduced red-blue splitting in the latter case. The opposite parity manifold of electrically strong field seeking substates is split by the lambda doubling energy Δ (d). Energy splitting contours are shown every 2 mK near the zero of a magnetic quadrupole trap for OH molecules [25] without E-field (e), and with $E = 150$ V/cm (f). The vectors give the quantization axis. Note the drastic widening of the lowest energy splitting contour.

Consider a magnetic quadrupole trap, where a weak-field seeking molecule remains trapped insofar as it adiabatically follows the field direction. Near the trap center, the direction changes most rapidly, causing loss. When electric field is added, it dominates in the trap center where the magnetic field is weakest. Quantization is maintained but the quantization axis does not rotate with the magnetic field. Further away from the trap center the molecule is then magnetically strong field seeking and is lost. To avoid loss, the molecule must switch from the vector sum quantization axis to the vector difference quantization axis, so as to remain magnetically weak field seeking despite the change in relative orientation of the fields. To be more precise, we define the relative orientation of the fields as the sign of $\phi = \vec{E} \cdot \vec{B}$. When ϕ is negative (positive), the trapped state must have the vector difference (sum) quantization axis, so that an increase in magnitude of the magnetic field increases its energy. Orientation changes whenever ϕ changes sign, i.e. where $\phi = 0$ which means $E \perp B$. This happens in a 2D region, since $\phi = 0$ is a contour level of the 3D scalar valued function ϕ.

We can quantify this intuitive picture by diagonalizing the molecular Hamiltonian in mixed fields to find the energy splitting between the well trapped substate and its spin-flip partner (Fig. 1a-c). The preceding quantization axis discussion suggests that spin-flips occur when crossing the $\phi = 0$ planar region, so we expect to find a correspondingly reduced energy splitting there, since this splitting acts as a barrier to spin-flips. This is indeed the case, compare panels (b) and (c). In fact, by series expanding the exact eigenenergies of OH, we find $H_{E \perp B}(B) \approx (\mu_B B)^3 \Delta^2/(d_E E)^4$, Δ the lambda doubling term. The Zeeman splitting is no longer linear, but cubic. This means that the splitting will be small in a much larger region than otherwise.

This observation allows us to develop a scaling law for the loss enhancement in a magnetic quadrupole trap. The Landau-Zener formula [29] allows calculation of a characteristic energy splitting κ below which spin-flips occur. κ grows with temperature and trap gradient, and is 5 MHz for 50 mK OH in our previous magnetic quadrupole [30]. We can approximate the spin-flip loss rate as the molecule flux through the ellipsoid where the energy splitting equals κ. E-field widens this ellipsoid into a broad, thin disk (Fig. 1e-f), whose radius is found by solving for B when $H_{E \perp B}(B) = \kappa$. Squaring and dividing by the original cross section gives the enhancement factor $\eta = (d_E E/\sqrt{\kappa\Delta})^{8/3}$. Thus E-fields beyond $\sqrt{\kappa\Delta}/d_E$ lead to almost cubic enhancements in spin-flip loss for OH (Tab. I). This new understanding modifies our interpretation of evaporation data for OH [20], especially at 5 mK where the loss rate is significantly enhanced by the E-fields used for RF knife purposes. The data do still show enhancements in normalized low-field density for light cuts from $45 - 30$ mK.

TABLE I. Enhancements and loss rates for OH with typical applied fields. Zero field values are equivalent to atomic spin-flip loss. E-field is required during evaporation and spectroscopy to open avoided crossings for $|e\rangle$ parity states [20, 25]. Background loss is 2 s^{-1}, experiment length 100 ms.

E (V/cm)	45 mK		5 mK		Purpose
	η	$\Gamma\,(s^{-1})$	η	$\Gamma\,(s^{-1})$	
0	1	0.02	1	1.3	Zero Field
300	5	0.1	9	11	Evaporation
550	17	0.3	40	50	Spectroscopy
3000	1000	19	1600	2000	Polarizing

Generalizing beyond OH, Hund's case (a) states exhibit reduced Zeeman splittings near $B = 0$ when $E \perp B$ that are not always cubic as for OH but satisfy $H_{E \perp B}(B) \propto (\mu_B B)^{2m_J}$. Only states with $m_J = 1/2$ retain a linear Zeeman splitting, but they are either not well trapped if $J = 1/2$ also, or they have avoided crossings with other states, see $|f, 1/2\rangle$ for OH in gray in Fig. 1(c). This bears out in all test Hamiltonians we have diagonalized, and can be understood intuitively as follows: the Zeeman effect is a perturbation on a Hamiltonian whose quantization axis, which defines the $|m_J\rangle$ quantum number, has already been set by the Stark effect. Normally the Zeeman effect would linearly split states according to $|m_J\rangle$, but from its perspective the states are superpositions $|m_J\rangle \pm |-m_J\rangle$ and do not split at all to first order. Only via perturbations of the eigenbasis itself is a Zeeman splitting achieved.

For Hund's case (b) states the electric and magnetic field couple to different parts of the molecule: the molecular rotation and the electron orbit/spin respectively. There is not any competition between quantization axes or any spin-flip loss enhancement and the Stark and Zeeman effects combine linearly regardless of field orientation [28]. However, no state is perfectly Hund's case (b), they always exhibit some degree of spin-rotation coupling, usually denoted by γ. This coupling resurrects quantization axes competition on the γ energy scale. Spin-flip loss can be enhanced by electric field to the extent that $\kappa < \gamma$. For all laser-cooled molecules and bialkalis thus far, γ is in the tens of MHz [21]. κ is generally much lower than the 5 MHz for OH, given our high temperature and tight trap, and thus spin-flip loss enhancement is important for Hund's case (b). Some Hund's case (b) states of yttrium oxide exhibit a protected substate that is magnetically trappable and spin-flip immune due to an interplay between hyperfine contributions and the spin-rotation coupling [**?**].

We can generalize to arbitrary geometries and consider methods to avoid the loss using a simple strategy: avoid $\mu_B B < d_E E$ where $E \perp B$. One way to achieve this is to trap with E-field and superpose B-field. The lambda doublet prevents flips in this configuration, but

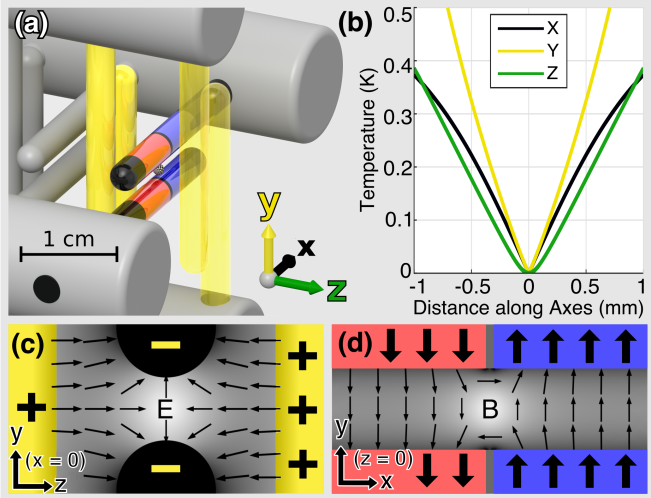

FIG. 2. The last six pins of our Stark decelerator [30] form the trap (a), which is 0.45 mK deep with trap frequency $\nu \approx 4$ kHz (b). Along y the trap is bounded by the 2 mm pin spacing. The yellow pins are positively charged while the central pin pair is grounded, which forms a 2D electric quadrupole trap with zero along the x-axis. This is shown for the $x = 0$ plane (c), with yellow pins artificially projected for clarity since they don't actually intersect the plane. The central pins are magnetized, with two domains each. Blue indicates magnetization along $+\hat{y}$, red along $-\hat{y}$. These domains produce a magnetic quadrupole trap with zero along the z-axis, shown in the $z = 0$ plane (d).

it correspondingly rounds the trap minimum, weakening confinement. Another option is to trap with both fields and keep zeros overlapped. This was once realized for OH with a superposed magnetic quadrupole and electric hexapole [31]. Such a scheme prevents spin-flip loss enhancement, but does not remove it entirely. It is also susceptible to misalignment induced loss enhancement. Another possibility is to use one field only. While this avoids spin-flip loss enhancement, any experiment which aims to make use of the doubly dipolar nature of molecules cannot accept this compromise.

We opt for a geometry that is distinct from these options: a pair of 2D quadrupole traps, one magnetic and the other electric, with orthogonal centerlines (Fig. 2). We achieve these fields in a geometry that matches our Stark decelerator [14]. This approach is similar to the Ioffe-Pritchard strategy [32], where a 2D magnetic quadrupole is combined with an axial magnetic dipole trap. While this successfully prevents spin-flip loss, axial and radial trapping interfere, resulting in significantly lower trap depths than the 3D quadrupole. We thwart this interference by using electric field for the third direction. Our geometry has $E \perp B$ in the planes $x \cdot y = 0$, and $\mu_B B < d_E E$ in a large cylinder surrounding the z-axis. However, by adding magnetic field $\vec{B} = B_{\text{coil}}\hat{z}$ along the centerline of the magnetic quadrupole with an external bias coil, a fully tunable scenario emerges.

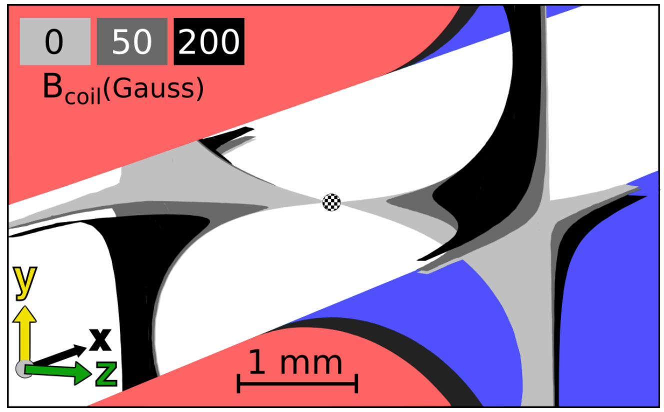

FIG. 3. Surfaces where spin-flips can occur ($E \perp B$, $\mu_B B < d_E E$) are shown for three values of B_{coil}. The magnetic pins are shown as in Fig. 2 for context. The very center of the trap is indicated; the cloud itself fits within about a 1 mm diameter.

Adding B_{coil} only slightly rounds the magnetic trapping potential, but it morphs the $E \perp B$ surface from a pair of planes into a hyperbolic sheet ($x \cdot y \propto B_{\text{coil}}$), pushing it away from the z-axis where the magnetic field is smallest. Thus small magnitudes of B_{coil} are sufficient to avoid loss. In Fig. 3, the surfaces where $E \perp B$ for several B_{coil} magnitudes are shown wherever the splitting is below the hopping threshold κ. The loss regions are always visible, but they are tuned too far away from the trap center to be accessed. The striking difference in molecule trap lifetime with and without B_{coil} can be seen in Fig. 4(a).

As a further confirmation of our model of the loss, we translate the magnetic pins along the $\hat{x}$ direction in their mounts to alter the surface where $E \perp B$ and compare experimental data against expectations (Fig. 4b). Qualitatively, this translation serves to disrupt the idealized 2D magnetic quadrupole by adding a small trapping field $\vec{B} \propto B' z\hat{z}$. This means that B_{coil} no longer directly tunes the magnetic field magnitude along the z-axis. Instead, B_{coil} must first overcome the slight trapping field, translating a point of zero field along the z-axis and eventually out of the trap. The point of zero magnetic field has $\mu_B B < d_E E$ and lies on the $\phi = \vec{E} \cdot \vec{B} = 0$ surface by definition, leading to strong loss unless it is aligned with the trap center, where E is also zero. This means that without B_{coil}, the loss should actually be a local minimum; as $|B_{\text{coil}}|$ is increased the loss should first worsen and then improve when the zero leaves the trap. This qualitative explanation correctly predicts the observed double well structure in population verses B_{coil}.

Quantitatively, we fit the family of curves (red, Fig. 4b) by integrating molecule flux weighted by Landau-Zener probability and Maxwell-Boltzmann population over the contorted surfaces where $E \perp B$ for each B_{coil} and pin translation. The computation is performed in COM-

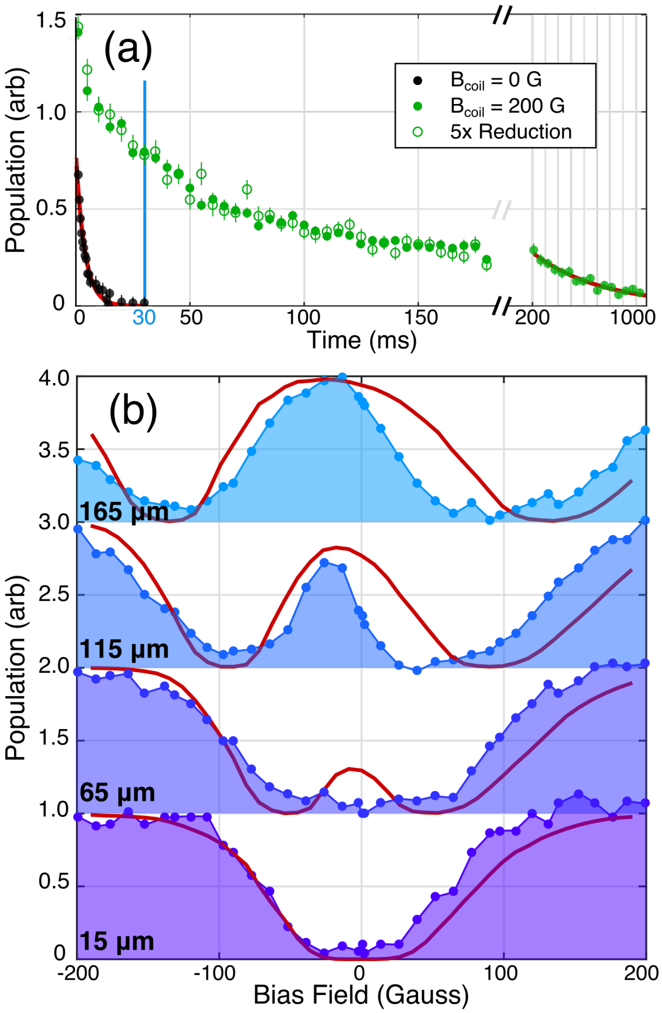

FIG. 4. Time traces (a) without bias field (black), with bias field (green dots), and with modulated density (green circles). One body fits (red) give loss rates of 200 s^{-1} without bias field and 2 s^{-1} with full bias field at long times, in agreement with our background gas pressure. At the fixed time 30 ms, population is shown as a function of both pin translation and bias field (b), for several values of pin translation, labeled relative to perfect alignment.

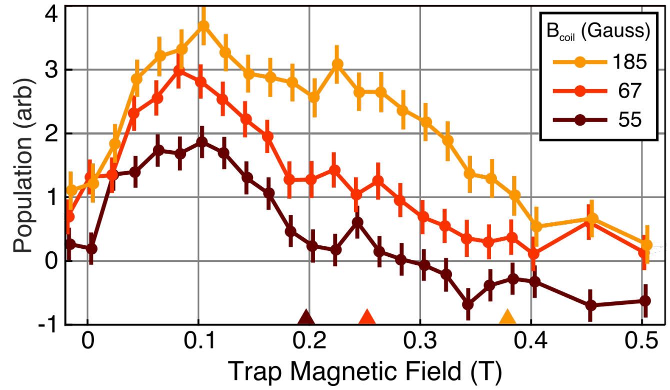

FIG. 5. Microwave spectroscopy. Increasing B_{coil} increases population and shifts its distribution toward higher fields. Triangles indicate the field at which a molecule can access loss regions for a given B_{coil}.

SOL, with cloud temperature as the only free parameter [33]. The asymmetry of the curves about $B_{\mathrm{coil}} = 0$ comes from a slight shift of the electric quadrupole field caused by an intentional bending of the last pin pair. This bend enhances laser induced fluorescence collection, our detection technique. The fitted temperature is in the $100 - 200$ mK range, larger than expected from our simulations, which already account for known losses [34]. This may relate to micro-discharges on the surfaces of the magnetic pins during the final deceleration pulse, since these specially manufactured pins are more difficult to polish. Various polishing strategies could overcome this limitation.

We further confirm our model using microwave spectroscopy (Fig. 5). The spectroscopy is performed as in our previous work [20], but with a microwave probe directly exciting free space modes of our vacuum chamber . It is seen that increasing B_{coil} increases population first at low fields and then at higher fields. This is consistent with our calculations of loss location (Fig. 3). In order to perform this spectroscopy, the trapping electric fields are switched off immediately prior to Zeeman specific microwave transfer pulses. Thus the results reflect the Zeeman potential energy only, which is related to the total potential energy in a complex way depending on the Stark energy and $E \cdot B$ at a given molecule location. Nonetheless, in the ensemble average the Zeeman and total potential energies should track one another, and the observed shift in population center is clear and in agreement with our expectation.

In the case of lowest applied magnetic field in Fig. 5, a negative going signal is observed. This indicates a build-up in an opposite parity state. Although the spin-flips we have discussed connect $|f, 3/2\rangle$ to $|f, -3/2\rangle$, the latter experiences various avoided crossings and remains weakly trapped. Its field-dressed state character varies, transitioning to $|e, 3/2\rangle$ at larger magnetic fields.

With loss removed, we observe a population dependent decay trend (Fig. 4a, green dots), suggestive of collisions. To test this, we implement a five-fold reduction in initial population and scale the resulting trend by five (green circles). If collisions had contributed, this new trend would decay less rapidly, but we observe no significant change. Our population reduction is achieved early during deceleration, with a microwave field that weakly couples opposite parities, giving a probability for molecules to be lost from the decelerator. This technique should not favor molecules that would end up in one part of the eventually trapped phase-space over another, and so the population distribution should be perturbed only by an overall scaling. Any other perturbation would be unlikely to yield the observed overlap. An alternative hypothesis for the decay trend is the existence of chaotic trap orbits with long escape times, as seen in [35].

This absence of collisions contrasts with our earlier evaporation work [20], which as we have mentioned still shows signatures of evaporation for light cuts. This could be attributed to a warmer initial temperature, reduced molecule number, or differences in trap geometry and loading. It is also possible that the spin-flip loss is playing a role even for the light evaporation cuts, although it is unclear how this could masquerade as a normalized low field density enhancement. Moving forward, we aim to continue with the spin-flip loss removed but increase the density so as to reattain the collisional regime, by means of several improvements [36, 37].

Molecule enhanced spin-flip loss arises in mixed electric and magnetic fields due to a competition between field quantization axes where $E \perp B$ and $\mu_B B < d_E E$. We conclusively demonstrate this effect and overcome it using our dual magnetic and electric quadrupole trap. Our explanation of the effect provides detailed predictions of how its location and magnitude ought to scale with bias field and trap alignment, which we experimentally verify. Our results correct existing predictions about molecular spin-flips in mixed fields and pave the way toward further improvements in molecule trapping and cooling.

We acknowledge the Gordon and Betty Moore Foundation, the ARO-MURI, JILA PFC, and NIST for their financial support. T.L. acknowledges support from the Alexander von Humboldt Foundation through a Feodor Lynen Fellowship. We thank J.L. Bohn and S.Y.T. van de Meerakker for helpful discussions. We thank Goulven Quéméner for his continued involvement in this research.

* Contributed equally.
† Present Address: 5. Physikalisches Institut and Center for Integrated Quantum Science and Technology (IQST), Universität Stuttgart, Pfaffenwaldring 57, 70569 Stuttgart, Germany

[1] L. D. Carr, D. DeMille, R. V. Krems, and J. Ye, New Journal of Physics **11**, 055049 (2009).
[2] S. A. Moses, J. P. Covey, M. T. Miecnikowski, B. Yan, B. Gadway, J. Ye, and D. S. Jin, Science **350**, 659 (2015).
[3] T. Takekoshi, L. Reichsöllner, A. Schindewolf, J. M. Hutson, C. R. Le Sueur, O. Dulieu, F. Ferlaino, R. Grimm, and H.-C. Nägerl, Physical Review Letters **113**, 205301 (2014).
[4] J. W. Park, S. A. Will, and M. W. Zwierlein, Physical Review Letters **114**, 205302 (2015).
[5] M. Guo, B. Zhu, B. Lu, X. Ye, F. Wang, R. Vexiau, N. Bouloufa-Maafa, G. Qu??m??ner, O. Dulieu, and D. Wang, Physical Review Letters **116**, 1 (2016).
[6] L. R. Liu, J. T. Zhang, Y. Yu, N. R. Hutzler, Y. Liu, T. Rosenband, and K.-K. Ni, , 1 (2017).
[7] M. T. Hummon, M. Yeo, B. K. Stuhl, A. L. Collopy, Y. Xia, and J. Ye, Physical Review Letters **110**, 143001 (2013).
[8] J. F. Barry, D. J. McCarron, E. B. Norrgard, M. H. Steinecker, and D. DeMille, Nature **512**, 286 (2014).
[9] V. Zhelyazkova, A. Cournol, T. E. Wall, A. Matsushima, J. J. Hudson, E. A. Hinds, M. R. Tarbutt, and B. E. Sauer, Physical Review A **89**, 053416 (2014).
[10] M. H. Steinecker, D. J. McCarron, Y. Zhu, and D. DeMille, ChemPhysChem **17**, 3664 (2016).
[11] B. Hemmerling, E. Chae, A. Ravi, L. Anderegg, G. K. Drayna, N. R. Hutzler, A. L. Collopy, J. Ye, W. Ketterle, and J. M. Doyle, Journal of Physics B: Atomic, Molecular and Optical Physics **49**, 174001 (2016).
[12] J. M. Doyle, J. D. Weinstein, R. DeCarvalho, T. Guillet, and B. Friedrich, Nature **395**, 148 (1998).
[13] H. L. Bethlem, G. Berden, and G. Meijer, Physical Review Letters **83**, 1558 (1999).
[14] J. R. Bochinski, E. R. Hudson, H. J. Lewandowski, G. Meijer, and J. Ye, Physical Review Letters **91**, 243001 (2003).
[15] E. Narevicius, A. Libson, C. G. Parthey, I. Chavez, J. Narevicius, U. Even, and M. G. Raizen, Physical Review Letters **100**, 093003 (2008).
[16] A. Wiederkehr, H. Schmutz, M. Motsch, and F. Merkt, Molecular Physics **110**, 1807 (2012).
[17] A. Prehn, M. Ibrügger, R. Glöckner, G. Rempe, and M. Zeppenfeld, Physical Review Letters **116**, 063005 (2016).
[18] Y. Liu, M. Vashishta, P. Djuricanin, S. Zhou, W. Zhong, T. Mittertreiner, D. Carty, and T. Momose, Physical Review Letters **118**, 093201 (2017).
[19] L. P. Parazzoli, N. J. Fitch, P. S. Zuchowski, J. M. Hutson, and H. J. Lewandowski, Physical Review Letters **106**, 1 (2011).
[20] B. K. Stuhl, M. T. Hummon, M. Yeo, G. Quéméner, J. L. Bohn, and J. Ye, Nature **492**, 396 (2012).
[21] G. Quéméner and J. L. Bohn, Physical Review A - Atomic, Molecular, and Optical Physics **93**, 1 (2016).
[22] A. L. Migdall, J. V. Prodan, W. D. Phillips, T. H. Bergeman, and H. J. Metcalf, Physical Review Letters **54**, 2596 (1985).
[23] W. Petrich, M. H. Anderson, J. R. Ensher, and E. A. Cornell, Physical Review Letters **74**, 3352 (1995).
[24] K. B. Davis, M. O. Mewes, M. R. Andrews, N. J. van Druten, D. S. Durfee, D. M. Kurn, and W. Ketterle, Physical Review Letters **75**, 3969 (1995).
[25] B. K. Stuhl, M. Yeo, B. C. Sawyer, M. T. Hummon, and J. Ye, Physical Review A **85**, 033427 (2012).
[26] M. Lara, B. L. Lev, and J. L. Bohn, Physical Review A **78**, 033433 (2008).
[27] B. K. Stuhl, M. Yeo, M. T. Hummon, and J. Ye, Molecular Physics **111**, 1798 (2013).
[28] J. L. Bohn and G. Quéméner, Molecular Physics **111**, 1931 (2013).
[29] J. R. Rubbmark, M. M. Kash, M. G. Littman, and D. Kleppner, Physical Review A **23**, 3107 (1981).
[30] B. C. Sawyer, B. K. Stuhl, D. Wang, M. Yeo, and J. Ye, Physical Review Letters **101**, 203203 (2008).
[31] B. C. Sawyer, B. L. Lev, E. R. Hudson, B. K. Stuhl, M. Lara, J. L. Bohn, and J. Ye, Physical Review Letters **98**, 1 (2007).
[32] D. E. Pritchard, Physical Review Letters **51**, 1336 (1983).
[33] Soure code: https://github.com/dreens/spin-flip-integration/.
[34] B. C. Sawyer, B. K. Stuhl, B. L. Lev, J. Ye, and E. R.

Hudson, European Physical Journal D **48**, 197 (2008).
[35] R. González-Férez, M. Iñarrea, J. P. Salas, and P. Schmelcher, Physical Review E **90**, 062919 (2014).
[36] U. Even, EPJ Techniques and Instrumentation **2**, 17 (2015).
[37] Y. Segev, N. Bibelnik, N. Akerman, Y. Shagam, A. Luski, M. Karpov, J. Narevicius, and E. Narevicius, Science Advances **3**, e1602258 (2017).